COMPOSITION, VERTICAL STRUCTURE, AND VARIABILITY OF THE NIGHT-SIDE IONOSPHERE OF MARS.

Z. Girazian, P. Mahaffy, M. Benna, M. Elrod, *NASA Goddard Space Flight Center, Greenbelt, MA, USA (zachary.r.rgirazian@nasa.gov)*, **R. Lillis,** *Space Sciences Laboratory, University of California Berkeley, CA, USA*.

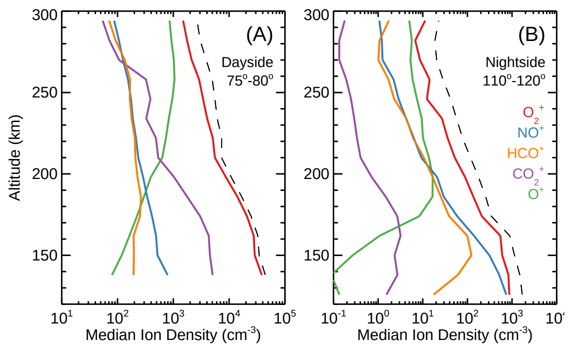

Figure 1: Median ion density profiles from the dayside (A) and the nightside (B). The dashed line is the total ion density.

Introduction

In the 1970's the Viking Landers obtained the first in situ observations of the dayside ionosphere of Mars. They showed that O_2^+ is the dominant ion and confirmed that photoionization by solar EUV radiation is the primary source of the dayside ionosphere (*Hanson et al.*, 1977). By contrast, the primary sources of the nightside ionosphere of Mars – day-to-night ion transport and particle precipitation – are not as well understood because in situ observations on the nightside were unavailable until 2014 when the Mars Atmosphere and Volatile EvolutioN (MAVEN) mission arrived at Mars (*Jakosky et al.*, 2015). Using observations from MAVEN's Neutral Gas and Ion Mass Spectrometer (NGIMS) (*Mahaffy et al.*, 2015), we describe the composition, vertical structure, and variability of the nightside ionosphere.

Composition of the Nightside Ionosphere

Figure 1 compares median ion density profiles from the dayside (SZA=75-80°) and the nightside (SZA=110-120°). On the dayside O_2^+ is the most abundant ion at all altitudes and CO_2^+ is the second most abundant ion below 200 km.

On the nightside O_2^+ is also the most abundant ion at all altitudes, but CO_2^+ is merely a minor species below 200 km where the composition is a mixture of O_2^+, HCO^+, and NO^+. This difference in the dayside and nightside composition is due to (1) the lack of a strong and continuous ionization source on the nightside and (2) ion-neutral chemical reactions that quickly convert CO_2^+ and O_2^+ into long-lived NO^+ and HCO^+ (e.g., *González-Galindo et al.*, 2013).

Vertical Structure of the Nightside Ionosphere

Figure 1 also shows that there are broad peaks in the CO_2^+, O^+, and HCO^+ density profiles around 190 km, 170 km, and 155 km, respectively. There is no distinct peak in the O_2^+ profile, although densities appear to be turning over below 150 km. An O_2^+ peak near this altitude is expected to form as a result of electron precipitation. There is no peak in the NO^+ density profile and NO^+ densities increase with decreasing altitude down to at least 130 km.

Long Term Variability in Nightside Densities

Figure 2 compares nightside median density profiles from December 2014 and July 2016. The O_2^+ and CO_2^+ densities were ~10 times larger in December 2014 than in July 2016. The larger nightside densities were most likely the result of an extended period of enhanced particle precipitation in December 2014, during which the MAVEN Solar Energetic Particle (SEP) instrument detected a major SEP electron event (*Lee et al.*, 2016, submitted to JGR). This event also produced the so-called "Christmas Lights" aurorae in the northern hemisphere (*Schneider et al.*, 2015).

Crustal Fields and Nightside Densities

Figure 3 shows nightside ion densities at 150 km as a function of geographic longitude. These observations come from a thin latitude band in the southern hemisphere near -75°. At this latitude there are strong crustal field regions at mid-longitudes between 100° and 250°.

Both the O_2^+ and CO_2^+ densities are smaller at mid-longitudes where the strongest crustal fields are located. These trends suggest that the electron precipitation and day-to-night ion transport is impeded by strong crustal fields. Such a behavior has also been suggested by previous observations (e.g., *Lillis and Brain*, 2013; *Dubinin et al.*, 2016).

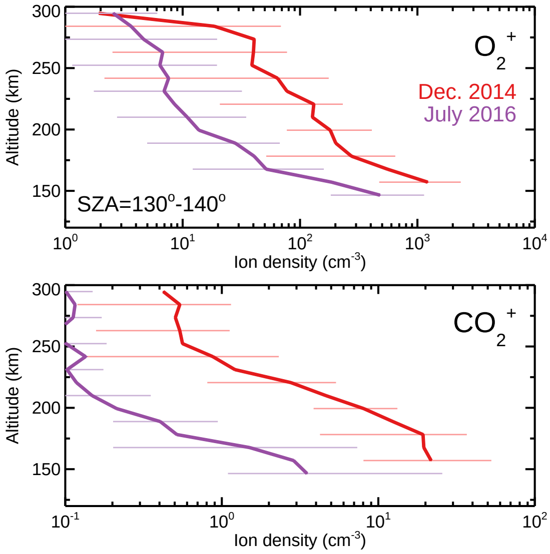

Figure 2: Median O_2^+ (top) and CO_2^+ (bottom) density profiles from two different periods of nightside observations. The red profiles are from observations obtained in December 2014 and the purple profiles are from observations obtained in July 2016. The densities were ∼10 times larger in December 2014, a time coinciding with a large solar energetic particle event at Mars.

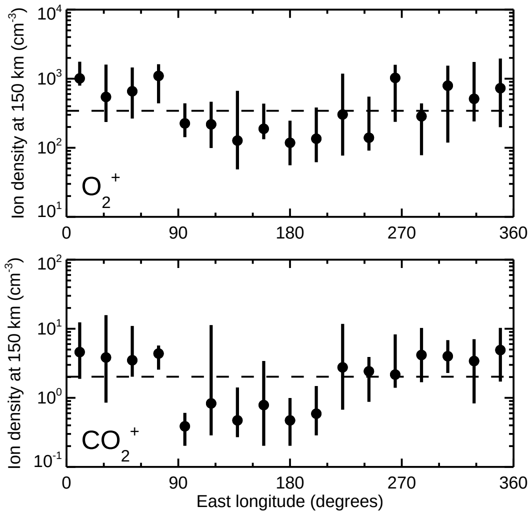

Figure 3: Median O_2^+ (top) and CO_2^+ (bottom) densities at 150 km as a function of geographic longitude. The circles show the median densities after binning in longitude, the error bars show the 25% and 75% quartiles, and the dashed line shows the median density of all the data points. The observations were obtained at southern latitudes near -75° where there are strong crustal field regions concentrated at east longitudes between 100°-250°. Both O_2^+ and CO_2^+ densities are smaller near these longitudes suggesting strong crustal fields impede particle precipitation and day-to-night ion transport.

References

Dubinin, E., M. Fraenz, A. D., and M. D., Martian Ionosphere observed by Mars Express. 1. Influence of the crustal magnetic fields, *Planet. Space Sci.*, *124*, 62–75, doi:10.1016/j.pss.2016.02.004, 2016.

González-Galindo, F., J.-Y. Chaufray, M. A. López-Valverde, G. Gilli, F. Forget, F. Leblanc, R. Modolo, S. Hess, and M. Yagi, Three-dimensional Martian ionosphere model: I. The photochemical ionosphere below 180 km, *J. Geophys. Res.*, *118*, 2105–2123, doi: 10.1002/jgre.20150, 2013.

Hanson, W. B., S. Sanatani, and D. R. Zuccaro, The martian ionosphere as observed by the Viking Retarding Potential Analyzers, *J. Geophys. Res.*, *82*, 4351–4363, doi:10.1029/JS082i028p04351, 1977.

Jakosky, B. M., J. M. Grebowsky, J. G. Luhmann, and D. A. Brain, Initial results from the MAVEN mission to Mars, *Geophys. Res. Lett.*, *42*, 8791–8802, doi: 10.1002/2015GL065271, 2015.

Lee, C. O., T. Hars, J. S. Halekas, P. Thiemann, P. Chamberlin, F. Eparvier, R. J. Lillis, D. E. Larson, P. A. Dunn, J. Gruesbeck, S. M. Curry, J. G. Luhmann, and B. M. Jakosky, MAVEN observations of the solar cycle 24 space weather conditions at Mars, submitted to this issue, *J. Geophys. Res.*, 2016.

Lillis, R. J., and D. A. Brain, Nightside electron precipitation at Mars: Geographic variability and dependence on solar wind conditions, *J. Geophys. Res.*, *118*, 3546–3556, doi:10.1002/jgra.50171, 2013.

Mahaffy, P. R., M. Benna, M. Elrod, R. V. Yelle, S. W. Bougher, S. W. Stone, and B. M. Jakosky, Structure and composition of the neutral upper atmosphere of Mars from the MAVEN NGIMS investigation, *Geophys. Res. Lett.*, *42*, 8951–8957, doi: 10.1002/2015GL065329, 2015.

Schneider, N. M., J. I. Deighan, S. K. Jain, A. Stiepen, A. I. F. Stewart, D. Larson, D. L. Mitchell, C. Mazelle, C. O. Lee, R. J. Lillis, J. S. Evans, D. Brain, M. H. Stevens, W. E. McClintock, M. S. Chaffin, M. Crismani, G. M. Holsclaw, F. Lefevre, D. Y. Lo, J. T. Clarke, F. Montmessin, and B. M. Jakosky, Discovery of diffuse aurora on Mars, *Science*, *350*, 0313, doi:10.1126/science.aad0313, 2015.